29th EPS Conference on Plasma Phys. and Contr. Fusion Montreux, 17-21 June 2002 ECA Vol. **26B**, P-1.072 (2002)

Simulation of Core Transport in ITER Plasmas with First-Principle-Based Transport Models

G. V. Pereverzev, G. Janeschitz[1], A. S. Kukushkin[2], V. S. Mukhovatov[3], G. W. Pacher[4], H. D. Pacher[5], A. R. Polevoi[3], O. V. Zolotukhin[2]

Max-Planck-Institut für Plasmaphysik, EURATOM Association, Garching, Germany
[1]Forschungszentrum Karlsruhe, Germany, [2]ITER JCT, Garching, Germany,
[3]ITER JCT, Naka, Japan, [4]Hydro Quebec (IREQ), Canada, [5]INRS Quebec, Canada

1. Introduction

In the last few years remarkable progress has been achieved in understanding transport processes in a tokamak. Several transport models based on theoretical considerations of the gradient driven turbulence have been developed and applied for modelling the core thermal transport in present-days tokamaks. This modelling demonstrated a reasonable agreement with many experimentally observed regimes in different tokamaks. It is commonly accepted now that the ion heat transport is governed by the ion temperature gradient and trapped electron mode (ITG/TEM) turbulence. Although, in general, the electron heat transport is described by these models with less accuracy also, in case of purely electron heating, some convincing results were recently obtained.

On the other hand, in spite of the same underlying physics, all existing theoretical models have also distinctive features and describe different tokamak regimes with noticeable scatter. This calls in question a predictive capability of these models for a tokamak-reactor. The objective of this study is to run presently available theoretical transport models for the plasma core under the same conditions and thus evaluate how significant the uncertainty in extrapolating existing models to future devices can be.

Although different models employed in this study explore basically the same gradient driven turbulence they differ in many details and in the final evaluation of the transport coefficients. It will be seen that this differences in approach results in a substantial differences of predictions for ITER.

2. Description of the transport model

Three ITG-based transport models, IFS/PPPL [1], GLF23 [2] and MMM95 [3] have been implemented in the 1.5D transport code Astra [5]. In our implementation, the main component of the MMM95 model is the Weiland transport model [4] which showed a good agreement with many present day tokamaks. All models provide electron and ion heat conductivity. However, the diffusion coefficient is not given by the IFS/PPPL model. In addition, most of interpretive simulations were so far concentrated on the energy transport alone while the particle transport is still much less studied. To conduct comparisons of different models under similar conditions and to employ only those features of transport models which are well verified we adopted the following simplified approach.

Heat conductivities for electron and ions were taken directly from the corresponding transport models while a simplified description for the particle diffusion was employed. This approach was verified against an extended set of ASDEX Upgrade and JET discharges and proved in reasonable agreement with the observations [6,7]. In this approach, the particle flux is presented as $\mathbf{\Gamma} = \mathbf{v}^{neo} n_e - (D_e^{neo} + D_e^{an})\nabla n_e$ with D_e^{neo} and $\mathbf{v}^{neo}$ being the neoclassical diffusion coefficient and the pinch velocity, respectively. The anomalous diffusion coefficient is taken as $D_e^{an} = 0.2(\chi_e^{an} + \chi_i^{an})$ assuming that the turbulence responsible for the energy transport causes also the particle transport. A feedback procedure was enabled for the density control. Influx of wall neutrals was set in such a way that the volume average electron density was maintained at the level of 10^{20} m^{-3}. Impurity composition and radial distribution were prescribed according to the reference ITER-FEAT scenario [8].

For the current density diffusion a conventional model with the neoclassical conductivity and bootstrap current has been used. A neutral beam driven current was included when the additional NB heating was applied.

An essential feature of the model is that the boundary conditions for the plasma density and for both temperatures were set inside the plasma, at the minor radius $a = 1.9$ m (in the mid-plane). This point is associated with the pedestal top. Outside the pedestal top, i.e. in the radial interval 1.9 m$< a <$ 2 m, plasma density and temperatures were prescribed. In all simulations presented below the boundary value $n_e(a = 1.9 \text{ m}) = 8 \times 10^{19}$ m^{-3} was assumed. The boundary conditions for the equilibrium solver and for the current density diffusion were set at the radius $a = 2$ m. This approach was employed in order to single out an uncertainty in description of the gradient zone at the plasma edge. This uncertainty requires treatment of the pedestal top temperature T_{ped} as an input parameter. Influence of T_{ped} on the plasma performance is a subject of study in this report.

3. Simulation results

The model described above was applied to ITER-FEAT standard parameters and the results are presented in Fig. 1. Here the dependences of the power in α−particles P_α are shown as functions of the temperature at the pedestal top for three different transport models. In this figure and all throughout this report results of the MMM95 model are shown in red, the GLF23 model in green and the IFS/PPPL model in blue. A substantial spread in predictions for different models is observed. It is seen that the reference value of $P_\alpha = 80$ MW for the multi-mode model can be achieved if the temperature at the pedestal top exceeds 4 keV. Adding 40 MW of NB heating (tangential injection of 1 MeV neutrals) reduces this threshold in the pedestal temperature down to 3 keV. The other two models give more pessimistic prediction of 5 keV for IFS/PPPL and nearly 6 keV and GLF23 model. These two models are also much less sensitive to auxiliary heating and their predictions hardly change if the heating is applied.

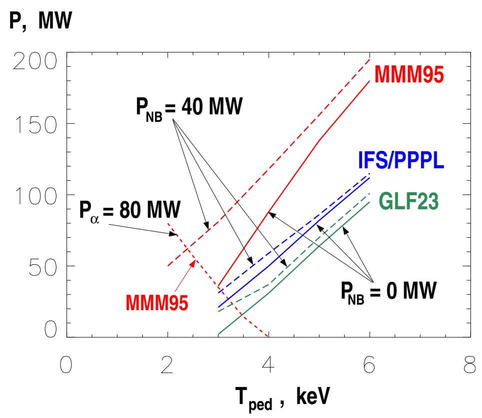

Fig. 1. Influence of the boundary temperature on the power in α-particles, P_α, for three different transport models. Solid curves show the case without additional heating, dashed curves show the case with 40 MW of NB heating. Dotted line shows the power of additional heating required for keeping the constant level of $P_\alpha = 80$ MW. For this case, the left scale shows P_{NB}.

This insensitivity stems from the stiff nature of the transport produced by the gradient driven turbulence, combining with the fixed boundary conditions in the simulation model. Under the latter constraint any attempt to rise the temperature gradient brings forth a strong enhancement of the transport thus minimising the overall system response. However, the stiffness of different models is rather different being the highest for IFS/PPPL model and the lowest for MMM-95. The relatively low stiffness of the MMM95 model allows to reduce the threshold $T_{ped} = 4$ keV if an additional heating is applied. This is illustrated by the dotted line in Fig. 1. The line shows the power of the NB heating which is needed to maintain the constant level of $P_\alpha = 80$ MW varying the boundary (pedestal) temperature.

The reaction of the system on the additional heating is illustrated by Fig. 2 where the ion temperature profiles with and without additional heating are shown for the three

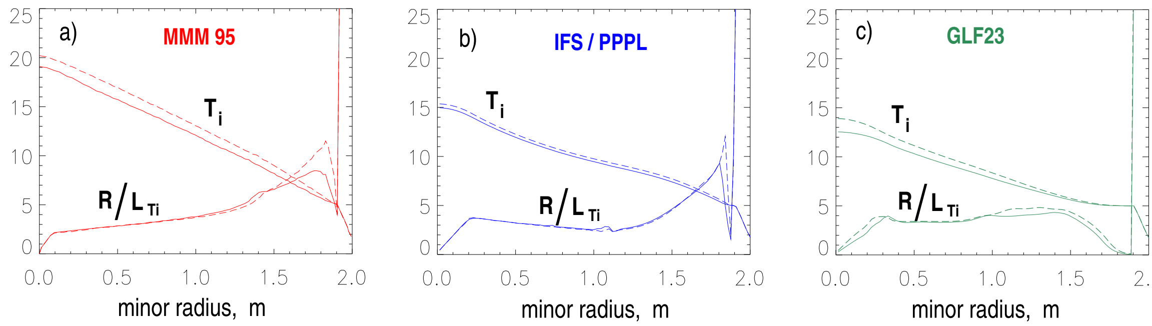

Fig. 2. Profiles of the ion temperature at the same boundary condition $T_{ped} = 5$ keV for different transport models. Radial dependencies of the dimensionless parameter R/L_{Ti} are also shown. The temperature is given in keV. The cases with (40 MW) and without additional heating are shown with dashed and solid lines, respectively.

models under consideration. The electron temperature profiles are very close to those of the ions and behave similar because of strong equipartition. Calculated temperature gradients are quite close to the critical gradients in all cases. Comparing cases with and without additional heating one can see that the stiffness increases with an increase in the temperature or, equivalently, in the heating power.

A distinctive feature of the GLF23 model is an extended region of ion temperature flattening at the plasma edge which is not observed for other models. This region is responsible for the relatively low fusion output calculated in the GLF23 model. It effectively shrinks the zone of high temperature and thus reduces the fusion power.[1] In the rest of the plasma, the critical gradients provided by this model could be relatively high and the transport is usually lower than in other models.

The last point addressed in this report is an influence of the adopted diffusion model on the simulation results. Because of the very low value of the neoclassical pinch very flat density profiles are obtained in all simulations. This is shown in Fig. 3. As mentioned above the flux of incoming neutral atoms Γ_N was adjusted in order to maintain the prescribed volume average electron density $< n_e >= 10^{20}$ m^{-3}. In spite of quite different ion temperature behaviour in the MMM95 and IFS/PPPL models the density profiles for these two models are very close to one another. The density profiles do not change noticeably when additional heating is applied. This observation confirms our assumption that the den-

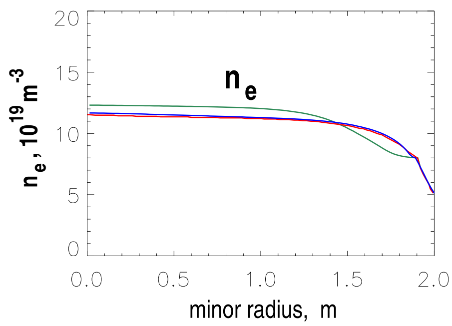

Fig. 3. Radial distribution of the electron density.

[1]Recently the GLF23 model was renormalised. This correction is not included in the results presented here. When applied, the renormalisation will improve predictions of the model.

sity diffusion model does not play a very significant role provided the average density can be held at the required level. In the GLF23 model, the density profile for GLF23 model shows the same flattening at the edge as the ion and electron temperatures. As a side remark, we note that, in most cases, the empirical anomalous diffusion coefficient $D_e^{an} = 0.2(\chi_e^{an} + \chi_i^{an})$ employed in our model is surprisingly close to the ion diffusion coefficient D_i^{an} provided by the GLF23 model. This property is not observed in the MMM95 model.

For the case shown in Fig. 3, the required flux through the last closed magnetic surface was $\Gamma_N = 1.4 \times 10^{22}$ s^{-1} for the IFS/PPPL model, 2.8×10^{22} s^{-1} for the MMM95 model and 5.2×10^{22} s^{-1} for the GLF23 model. A value of the neutral influx is directly related to a diffusivity at the plasma edge and therefore the GLF23 model requires a very high neutral flux. The parameter Γ_N is also sensitive to a width of the pedestal zone and to the plasma density distribution outside the pedestal top. Detailed modelling of the divertor plasmas [9] in ITER shows that the neutral flux through a separatrix due to recycling cannot exceed 10^{22} s^{-1}. Although a conclusive decision is beyond the accuracy of our approach it provides strong evidences that the recycling process alone will be insufficient for maintaining the plasma density at the level of $< n_e > = 10^{20}$ m^{-3}. On the other hand, this level cannot be reduced significantly because this will result in a corresponding reduction of the fusion power. Most probably, this means that a core plasma fuelling with pellets will be needed for ITER operation at high density.

4. Conclusions

The particle and energy balance in the plasma core were simulated making use of the three different theory based transport models implemented in the transport code ASTRA. In this modelling, we considered a plasma temperature at the pedestal top T_{ped} as an input parameter. It has been found that the most optimistic is the MMM95 model. At $T_{ped} \geq 3.5$ keV, this model predicts a capability of ITER operation with $Q > 10$. For the same fusion power, almost independent of Q, the IFS/PPPL and GLF23 models require at the pedestal top 5 keV and 5.5 keV, respectively.

All models show a stable burning phase once the ignition is achieved. All three models exhibit rather high stiffness and keep a temperature gradient very close to the critical one. Nevertheless, the response of the MMM95 model on auxiliary heating allows control of the fusion power in a noticeably wider range than the two other models.

Although a model of the pedestal zone was not implemented in the simulations presented here the conclusion can be drawn that a pellet injection could be a prerequisite in obtaining high density and high performance ($Q > 15$) operational regimes in ITER.

References

[1] M. Kotschenreuther, W. Dorland et al., Phys. Plasmas **2** (1995) 2381.
[2] R. E. Waltz, G. M. Staebler et al., Phys. Plasmas **4** (1997) 2482.
[3] G. Bateman, A. H. Kritz et al., Phys. Plasmas **5** (1998) 1793.
[4] J. Weiland, Collective Modes in Inhomogeneous Plasma, IOP, Bristol, 1999.
[5] G. V. Pereverzev and P. N. Yushmanov, IPP Report 5/98, February 2002.
[6] J. Stober, C. Fuchs et al., Nuclear Fusion **41** (2001) 1535.
[7] G. Janeschitz, G. W. Pacher et al., Plasma Phys. Control. Fusion **44** (2002) A459.
[8] ITER-FEAT Outline Design Report, ITER EDA Documentation Series No.18, IAEA, Vienna, 2001, p.5-51.
[9] A. S. Kukushkin and H. D. Pacher, Plasma Phys. Control. Fusion **44** (2002) 1.